ELSEVIER

Finite Elements in Analysis and Design 19 (1995) 115–129

FINITE ELEMENTS IN ANALYSIS AND DESIGN

The solution of axisymmetric problems near singular points and computation of stress intensity factors

Zohar Yosibash*, Barna Szabó

Center for Computational Mechanics, Washington University, Campus Box 1129, St. Louis, MO 63130, USA

Abstract

The computation of the stress intensity factors for axially symmetric domains, in the vicinity of singular points in the framework of linear elastostatics, is presented. It is shown that the decomposition of the solution in the neighborhood of *any* singular point, in an axisymmetric domain, is identical to the decomposition corresponding to plane strain condition, and an extraction vector, to be used in conjunction with the contour integral method and the *p*-version of the finite element method, is developed for crack singularities. Although the contour integral is shown to be path dependent for axisymmetric 2-D domains, in the limiting case it is valid for the computation of the crack stress intensity factors. Numerical examples support our analysis, extending the application of the superconvergent contour integral in conjunction with the *p*-version of the finite element method to the axisymmetric crack case.

1. Introduction

The axially symmetric elastostatic problem can be reduced to a system of two partial differential equations and solved on a two-dimensional (2-D) domain which represents the generating section of the axially symmetric body. Although the reduced problem is formulated on a 2-D domain, special treatment is required to find its solution in the vicinity of singular points.

In the case of a purely 2-D problem (plane strain or plane stress), we may use the zooming principle to examine the solution in the vicinity of the singular point, such that no length parameter which characterizes the solution domain is apparent. In this case, the solution can be expanded in the form [1]

$$\boldsymbol{u} = \sum_{i=1}^{I} \sum_{m=0}^{M} C_{im}\, r^{\alpha_i}\, \ln^m(r)\, \boldsymbol{f}_{im}(\theta) + \boldsymbol{u}^*(r,\theta), \tag{1}$$

where r and θ are polar coordinates centered on the singular point, $\boldsymbol{u}^*$ is a smoother function than the terms in the sum, $\boldsymbol{f}_{im}(\theta)$ are piecewise analytic vector functions, and C_{im} are the generalized stress intensity factors (GSIFs). $\boldsymbol{f}_{im}(\theta)$ and α_i are *eigenpairs*. The value of $\partial \boldsymbol{u}/\partial r$ is unbounded as r approaches zero for $\alpha_i < 1$. For a detailed discussion on the decomposition of the solution in the vicinity of singular points we refer to [1–5].

* Corresponding author.

SSDI 0 1 6 8 - 8 7 4 X(94)0 0 0 6 1 - 1

Reliable computation of the GSIFs is of great practical importance, because failure theories directly or indirectly involve these coefficients. However, computation of the GSIFs requires that the eigenpairs be known. These eigenpairs may be computed numerically.

In the 2-D axisymmetric problems, a characteristic length, which is the distance of the singular point from the axisymmetric axis, denoted by ρ_s, appears in the formulation which determine the eigenpairs. As a result, we show in Section 2 that the decomposition of the solution in the form of Eq. (1) holds true only in the limit with respect to $r/\rho_s \to 0$. This is shown by a method based on the Steklov formulation. Details on the Steklov formulation are available in [3, 4].

For isotropic axisymmetric problems, it has been shown in [6] that in the limit $r/\rho_s \to 0$, the eigenpairs are similar to those corresponding to plane-strain situation. The analysis in [6] is based on Love's stress function. We use the Steklov formulation to generalize this theorem, proving that the solution associated with the 2-D axisymmetric problem, in the vicinity of *any* singular point, can be expanded in terms of eigenpairs *identical* to these associated with the plane strain condition over the same 2-D domain.

Once the eigenpairs are found, the GSIFs may be extracted using various numerical methods. One of the most efficient methods to extract the GSIFs for cracked configurations is the contour integral method (CIM) first introduced in [7], and incorporated for 2-D elasticity in [8]. For detailed discussion on the CIM we refer to [7–9], where it has been shown that the method yield superconvergent results. We hereby demonstrate that the CIM becomes *path dependent* in the case of axisymmetric problems. It is also shown, however, that the CIM can be modified such that it becomes applicable to axisymmetric problems, and can be used for the extraction of the stress intensity factors from finite element solutions. An auxiliary function vector, called the extraction function vector, is constructed for use in conjunction with the CIM, and the p-version of the finite element method is utilized in the extraction of these crack GSIFs for axisymmetric problems.

Numerical results, demonstrating the results of the analysis, are presented in Section 3. The GSIF is calculated for three axisymmetric domains and compared to the exact values obtained by analytical methods (when available).

2. Decomposition of the solution in the vicinity of a singular point and extraction functions

Consider the generating section Ω of an axially symmetric domain shown in Fig. 1, where z is the axisymmetric axis and ρ is the radial distance from it. Denote by Γ_1 and Γ_2 the boundaries of a reentrant corner in Ω, such that Γ_1 and Γ_2 intersect in the singular point (ρ_s, z_s). We define Ω_R as the subdomain $\Omega \cap S_R$, where $S_R \equiv \{(\rho,z) \,|\, (\rho-\rho_s)^2+(z-z_s)^2 \leqslant R^2\}$. $\Gamma_3 \subset \Omega$ is defined as $\{(\rho,z) \,|\, (\rho-\rho_s)^2+(z-z_s)^2 = R^2\} \cap \Omega$. The polar coordinate system r, θ is located in the singular point (ρ_s, z_s). The displacements and traction vectors in the ρ and z directions will be denoted by $\boldsymbol{u} \stackrel{\text{def}}{=} \{u_\rho, u_z\}^T$ and $\boldsymbol{T} \stackrel{\text{def}}{=} \{T_\rho, T_z\}^T$, respectively.

The generalized (weak) form of the axially symmetric problem of elasticity is formulated as follows (see Eq. (5.72) in [9]):

$$\text{Seek } \boldsymbol{u} \in H^1(\Omega_R) \times H^1(\Omega_R) \quad \text{such that } \mathscr{B}(\boldsymbol{u}, \boldsymbol{v}) = \mathscr{F}(\boldsymbol{v}) \quad \forall \boldsymbol{v} \in H^1(\Omega_R) \times H^1(\Omega_R), \tag{2}$$

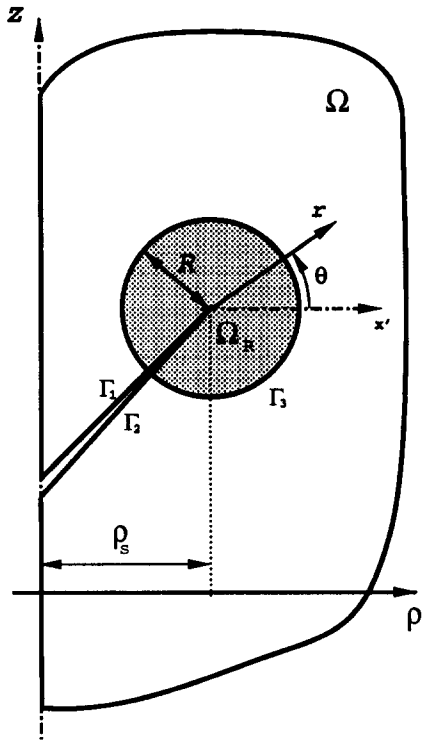

Fig. 1. The domain and notation.

where:

$$\mathscr{B}(\boldsymbol{u},\boldsymbol{v}) = \int\int_{\Omega_R} ([D]\{v\})^{\mathrm{T}}\,[E][D]\{u\}\rho\,\mathrm{d}\rho\,\mathrm{d}z \tag{3}$$

$$\mathscr{F}(\boldsymbol{v}) = \int_{\partial\Omega_R} (T_\rho v_\rho + T_z v_z)\rho\,\mathrm{d}s \equiv \sum_{i=1}^{2} \int_{\Gamma_i} \{v_\rho,\, v_z\} \begin{Bmatrix} T_\rho \\ T_z \end{Bmatrix} \rho\,\mathrm{d}s + \int_{\Gamma_3} \{v_\rho,\, v_z\} \begin{Bmatrix} T_\rho \\ T_z \end{Bmatrix} \rho\,\mathrm{d}s \tag{4}$$

and

$$[D] \overset{\text{def}}{=} \begin{bmatrix} \partial/\partial\rho & 0 \\ 1/\rho & 0 \\ 0 & \partial/\partial z \\ \partial/\partial z & \partial/\partial\rho \end{bmatrix}, \tag{5}$$

for isotropic domains $[E]$ is given by

$$[E] \overset{\text{def}}{=} \frac{E}{(1+\nu)(1-2\nu)} \begin{bmatrix} (1-\nu) & \nu & \nu & 0 \\ \nu & (1-\nu) & \nu & 0 \\ \nu & \nu & (1-\nu) & 0 \\ 0 & 0 & 0 & (1-2\nu)/2 \end{bmatrix}.$$

Assume that in Ω_R $\boldsymbol{u}$ can be expanded in terms of eigenpairs as follows (the $\ln r$ terms may appear in some special cases which we do not address here):

$$\boldsymbol{u} = r^{\alpha} \begin{Bmatrix} f(\theta) \\ g(\theta) \end{Bmatrix}. \tag{6}$$

On the boundaries Γ_1 and Γ_2 we assume the following homogeneous boundary conditions:

$$\begin{Bmatrix} T_\rho \\ T_z \end{Bmatrix} = - \begin{Bmatrix} u_\rho k_i^{(u_\rho)}/k_i^{(T_\rho)} \\ u_z k_i^{(u_z)}/k_i^{(T_z)} \end{Bmatrix} \quad \text{on } \Gamma_i, \ i = 1,2, \tag{7}$$

where $k_i^{(u_\rho)}$, $k_i^{(T_\rho)}$, $k_i^{(u_z)}$, and $k_i^{(T_z)}$ are constants. If $k_i^{(T_\rho)} = 0$ or $k_i^{(T_z)} = 0$, we omit this boundary condition and restrict the space in which $\boldsymbol{u}$ and $\boldsymbol{v}$ lie to be the one given by $\hat{H}^1(\Omega_R) \times \hat{H}^1(\Omega_R) \stackrel{\text{def}}{=} \{\boldsymbol{u} \mid \boldsymbol{u} \in H^1(\Omega_R) \times H^1(\Omega_R), \boldsymbol{u} = 0 \text{ on } \Gamma_i\}$. On the boundary Γ_3 the following relationship holds:

$$\begin{Bmatrix} T_\rho \\ T_z \end{Bmatrix} = [B]\{\sigma\} = [B][E][D]\{u\}, \quad [B] = \begin{bmatrix} \cos\theta & 0 & 0 & \sin\theta \\ 0 & 0 & \sin\theta & \cos\theta \end{bmatrix}, \tag{8}$$

For the case where x' is the same direction as ρ we have

$$\rho = \rho_s + r\cos\theta, \qquad z = \rho_s + r\sin\theta. \tag{9}$$

When x' is in the opposite direction to ρ such as, for example, when a crack is originating at the perimeter then,

$$\rho = \rho_s - r\cos\theta, \qquad z = \rho_s - r\sin\theta.$$

So that, in both cases

$$\begin{Bmatrix} \dfrac{\partial}{\partial\rho} \\ \dfrac{\partial}{\partial z} \end{Bmatrix} = \begin{bmatrix} \cos\theta & -\dfrac{1}{r}\sin\theta \\ \sin\theta & \dfrac{1}{r}\cos\theta \end{bmatrix} \begin{Bmatrix} \dfrac{\partial}{\partial r} \\ \dfrac{\partial}{\partial\theta} \end{Bmatrix}, \tag{10}$$

and [D] becomes

$$[D] = \begin{Bmatrix} \cos\theta\dfrac{\partial}{\partial r} - \dfrac{1}{r}\sin\theta\dfrac{\partial}{\partial\theta} & 0 \\ 1/(\rho_s \pm r\cos\theta) & 0 \\ 0 & \sin\theta\dfrac{\partial}{\partial r} + \dfrac{1}{r}\cos\theta\dfrac{\partial}{\partial\theta} \\ \sin\theta\dfrac{\partial}{\partial r} + \dfrac{1}{r}\cos\theta\dfrac{\partial}{\partial\theta} & \cos\theta\dfrac{\partial}{\partial r} - \dfrac{1}{r}\sin\theta\dfrac{\partial}{\partial\theta} \end{Bmatrix}, \tag{11}$$

therefore $[D]\{u\}$ can be written as

$$[D]\{u\} = \frac{1}{r}\begin{Bmatrix} \alpha\cos\theta - \sin\theta\dfrac{\partial}{\partial\theta} & 0 \\ r/(\rho_s \pm r\cos\theta) & 0 \\ 0 & \alpha\sin\theta + \cos\theta\dfrac{\partial}{\partial\theta} \\ \alpha\sin\theta + \cos\theta\dfrac{\partial}{\partial\theta} & \alpha\cos\theta - \sin\theta\dfrac{\partial}{\partial\theta} \end{Bmatrix}\{u\}. \tag{12}$$

Substituting (7)–(9) and (12) into (4) we obtain

$$\mathscr{F}\{v\} = -R\sum_{i=1}^{2}\int_{\Gamma_i}\{v\}^{\mathrm{T}}\begin{Bmatrix} u_\rho k_i^{(u_\rho)}/k_i^{(T_\rho)} \\ u_z k_i^{(u_z)}/k_i^{(T_z)} \end{Bmatrix}(\rho_s/R \pm (r/R)\cos\theta)\mathrm{d}s$$

$$+\alpha R\int_\theta \{v\}^{\mathrm{T}}[B][E]\begin{Bmatrix} \cos\theta & 0 \\ 0 & 0 \\ 0 & \sin\theta \\ \sin\theta & \cos\theta \end{Bmatrix}\{u\}(\rho_s/R \pm \cos\theta)\mathrm{d}\theta$$

$$+R\int_\theta \{v\}^{\mathrm{T}}[B][E]\begin{Bmatrix} -\sin\theta\dfrac{\partial}{\partial\theta} & 0 \\ 1/(\rho_s/R \pm \cos\theta) & 0 \\ 0 & \cos\theta\dfrac{\partial}{\partial\theta} \\ \cos\theta\dfrac{\partial}{\partial\theta} & -\sin\theta\dfrac{\partial}{\partial\theta} \end{Bmatrix}\{u\}(\rho_s/R \pm \cos\theta)\mathrm{d}\theta. \tag{13}$$

To simplify our discussion let us assume Dirichlet boundary conditions on Γ_1 and Γ_2, such that the first term in (13) can be omitted. In this case, after multiplying left and right hand sides of (2) by R/ρ_s, the weak form of the Steklov problem is given as follows:

Seek $\alpha \in \mathscr{C}$, and $0 \neq \boldsymbol{u} \in \hat{H}^1(\Omega_R) \times \hat{H}^1(\Omega_R)$ such that $\forall \boldsymbol{v} \in \hat{H}^1(\Omega_R) \times \hat{H}^1(\Omega_R)$,

$$\int_0^R\int_\theta([D]\{v\})^{\mathrm{T}}[E][D]\{u\}(1 \pm (r/\rho_s)\cos\theta)r\,\mathrm{d}r\,\mathrm{d}\theta$$

$$-\int_\theta \{v\}^{\mathrm{T}}[B][E]\begin{Bmatrix} -\sin\theta\dfrac{\partial}{\partial\theta} & 0 \\ 1/(\rho_s/R \pm \cos\theta) & 0 \\ 0 & \cos\theta\dfrac{\partial}{\partial\theta} \\ \cos\theta\dfrac{\partial}{\partial\theta} & -\sin\theta\dfrac{\partial}{\partial\theta} \end{Bmatrix}\{u\}(1 \pm (R/\rho_s)\cos\theta)\mathrm{d}\theta$$

$$= \alpha \int_\theta \{v\}^{\mathrm{T}} [B][E] \begin{Bmatrix} \cos\theta & 0 \\ 0 & 0 \\ 0 & \sin\theta \\ \sin\theta & \cos\theta \end{Bmatrix} \{u\}(1 \pm (R/\rho_s)\cos\theta)\mathrm{d}\theta. \tag{14}$$

This is an eigenvalue problem which can be solved by means of the finite element method.

Remark 1. The decomposition of the solution in the vicinity of singular points into an asymptotic series of eigenpairs of the form (6) is valid only for $R/\rho_s \ll 1$, and as $R/\rho_s \to 0$ the fewer terms in the asymptotic expansion are needed for an accurate solution.

Notice that $r < R$, so that in the limit as $(R/\rho_s) \to 0$ (14) takes the form

$$\int\int_{\Omega_R} \left([\hat{D}]\{v\}\right)^{\mathrm{T}} [E][\hat{D}]\{u\} r \,\mathrm{d}r\,\mathrm{d}\theta - \int_\theta \{v\}^{\mathrm{T}} [B][E] \begin{Bmatrix} -\sin\theta\dfrac{\partial}{\partial\theta} & 0 \\ 0 & 0 \\ 0 & \cos\theta\dfrac{\partial}{\partial\theta} \\ \cos\theta\dfrac{\partial}{\partial\theta} & -\sin\theta\dfrac{\partial}{\partial\theta} \end{Bmatrix} \{u\}\,\mathrm{d}\theta$$

$$= \alpha \int_\theta \{v\}^{\mathrm{T}} [B][E] \begin{Bmatrix} \cos\theta & 0 \\ 0 & 0 \\ 0 & \sin\theta \\ \sin\theta & \cos\theta \end{Bmatrix} \{u\}\,\mathrm{d}\theta, \tag{15}$$

where

$$[\hat{D}] = \begin{Bmatrix} \cos\theta\dfrac{\partial}{\partial r} - \dfrac{1}{r}\sin\theta\dfrac{\partial}{\partial\theta} & 0 \\ 0 & 0 \\ 0 & \sin\theta\dfrac{\partial}{\partial r} + \dfrac{1}{r}\cos\theta\dfrac{\partial}{\partial\theta} \\ \sin\theta\dfrac{\partial}{\partial r} + \dfrac{1}{r}\cos\theta\dfrac{\partial}{\partial\theta} & \cos\theta\dfrac{\partial}{\partial r} - \dfrac{1}{r}\sin\theta\dfrac{\partial}{\partial\theta} \end{Bmatrix}.$$

The Steklov formulation in the limiting case given by (15) is identical to the one corresponding to the plane-strain formulation problem presented in [3].

Remark 2. The Steklov formulation (15) is applicable to any singular point resulting from reentrant corners, multimaterial interfaces, or abrupt changes in boundary condition.

Therefore, we may conclude that the eigenpairs for the 2-D axisymmetric problem are identical to the ones corresponding to plane-strain problem over the same domain. This result is consistent with Sneddon's analysis for a loaded penny shaped crack in an infinite body presented in [10], and Zak's

analysis presented in [6]. Consequently, the extraction function vector, denoted by $\boldsymbol{w} = \{w_\rho, w_z\}^T$, is also identical to the one already given in [9, Ch. 12] for the plane-strain problem.

Eq. (14) was numerically solved using a p-version finite element formulation as described in [4]. Numerical results support our analysis conclusions, and the eigenpairs converge to those associated with the plane-strain case as $R/\rho_s \to 0$.

2.1. Application of the contour integral method to axisymmetric problems

The contour integral $I_\Gamma(\boldsymbol{u}, \boldsymbol{w})$ along any path beginning at Γ_1 and ending on Γ_2:

$$I_\Gamma(\boldsymbol{u}, \boldsymbol{w}) \stackrel{\text{def}}{=} \int_\Gamma \left[\left(T_n^{(u)} w_n + T_t^{(u)} w_t\right) - \left(T_n^{(w)} u_n + T_t^{(w)} u_t\right)\right] \mathrm{d}s, \tag{16}$$

presented in (12.23) in [9] is shown to be independent of Γ for *purely 2-D problems*. Here, T stands for normal or tangential traction computed from the displacement vector $\boldsymbol{u}$ or the extraction vector $\boldsymbol{w}$, while n and t represent the normal and tangential components.

To apply the contour integral for axisymmetric problems, the traction vectors corresponding to $\boldsymbol{w}$ and $\boldsymbol{u}$ have to be calculated. Therefore, the stress components σ_ρ, σ_z and $\tau_{\rho z}$, have to be evaluated first. Note that σ_θ is not of interest because the traction vector is independent of it. The stress–displacement relationships in the axisymmetric case (corresponding to $\boldsymbol{w}$ for example) are:

$$\begin{aligned}
\sigma_\rho^{(w)} &= E_{11}\frac{\partial w_\rho}{\partial \rho} + E_{12}\frac{\partial w_z}{\partial z} + E_{13}\frac{w_\rho}{\rho},\\
\sigma_z^{(w)} &= E_{21}\frac{\partial w_\rho}{\partial \rho} + E_{22}\frac{\partial w_z}{\partial z} + E_{23}\frac{w_\rho}{\rho},\\
\tau_{\rho z}^{(w)} &= E_{44}\left(\frac{\partial w_\rho}{\partial z} + \frac{\partial w_z}{\partial \rho}\right).
\end{aligned} \tag{17}$$

Substituting (6) into (8), then changing to normal–tangential coordinate system, we obtain the traction components corresponding to the ith eigenpair as

$$\begin{aligned}
T_{n(i)}^{(u)} &= r^{\alpha_i - 1}\left[\Upsilon_i^{(u)}(\theta) + (r/\rho)\upsilon_i^{(u)}(\theta)\right],\\
T_{t(i)}^{(u)} &= r^{\alpha_i - 1}\left[\Psi_i^{(u)}(\theta) + (r/\rho)\psi_i^{(u)}(\theta)\right],\\
T_{n(i)}^{(w)} &= r^{-\alpha_i - 1}\left[\Upsilon_i^{(w)}(\theta) + (r/\rho)\upsilon_i^{(w)}(\theta)\right],\\
T_{t(i)}^{(w)} &= r^{-\alpha_i - 1}\left[\Psi_i^{(w)}(\theta) + (r/\rho)\psi_i^{(w)}(\theta)\right],
\end{aligned} \tag{18}$$

where $\Upsilon_i^{(u)}$, $\Upsilon_i^{(w)}$, $\Psi_i^{(u)}$, $\Psi_i^{(w)}$, $\upsilon_i^{(u)}$, $\upsilon_i^{(w)}$, $\psi_i^{(u)}$ and $\psi_i^{(w)}$ are all smooth functions of θ containing trigonometric functions and material constants. The functions $\upsilon_i^{(u)}$, $\upsilon_i^{(w)}$, $\psi_i^{(u)}$ and $\psi_i^{(w)}$ do not appear in the purely 2-D cases, but we shall show that they disappear as $R/\rho_s \to 0$.

Once we obtained all components required for evaluating the contour integral, we proceed by modifying it for the case of axisymmetric 2-D domain. Following the analysis presented in [9, Ch. 12], we

obtain the CIM integral to be formulated as in the 2-D case, except that ds must be replaced by (ρ/ρ_s)ds, namely

$$I^A_\Gamma(\boldsymbol{u},\boldsymbol{w}) = \int_\Gamma \left[\left(T^{(u)}_n w_n + T^{(u)}_t w_t\right) - \left(T^{(w)}_n u_n + T^{(w)}_t u_t\right)\right](\rho/\rho_s)\mathrm{d}s. \tag{19}$$

Clearly, $I^A_\Gamma(\boldsymbol{u},\boldsymbol{w})$ is no longer path independent. In the following, however, we prove that on a circular path Γ, of radius R, in the limit $R/\rho_s \to 0$ we obtain $I^A_\Gamma \to I_\Gamma$, and path independency is recovered for the axisymmetric case under the restrictive assumption that $\rho_s \gg R$.

Let us examine a typical term in the expression for I^A_Γ, which will be denoted by $I^A_{\Gamma(ij)}$ and corresponds to the ith term of T_n and the jth term of w_n:

$$I^A_{\Gamma(ij)} = \int_\Gamma T^{(u)}_{n(i)} w_{n(j)}(\rho/\rho_s)\mathrm{d}s = \int_\Gamma r^{\alpha_i-\alpha_j-1}\left[\Upsilon^{(u)}_i(\theta) + (r/\rho)\upsilon^{(u)}_i(\theta)\right] f_j(\theta)(\rho/\rho_s)\mathrm{d}s. \tag{20}$$

On a circular path of radius R, this term becomes

$$I^A_{\Gamma(ij)} = R^{\alpha_i-\alpha_j}\left[\int_\theta \Upsilon^{(u)}_i(\theta) f_j(\theta)(1 \pm (R/\rho_s)\cos(\theta))\,\mathrm{d}\theta + (R/\rho_s)\int_\theta \upsilon^{(u)}_i(\theta) f_j(\theta)\mathrm{d}\theta\right]. \tag{21}$$

In the limit $R/\rho_s \to 0$ we have $(1 \pm (R/\rho_s)\cos(\theta)) \to 1$ so (21) becomes

$$I^A_{\Gamma(ij)} = R^{\alpha_i-\alpha_j}\left[\int_\theta \Upsilon^{(u)}_i(\theta) f_j(\theta)\mathrm{d}\theta + (R/\rho_s)\int_\theta \upsilon^{(u)}_i(\theta) f_j(\theta)\mathrm{d}\theta\right] \tag{22}$$

and because $\int_\theta \Upsilon^{(u)}_i(\theta) f_j(\theta)\mathrm{d}\theta$ and $\int_\theta \upsilon^{(u)}_i(\theta) f_j(\theta)\mathrm{d}\theta$ are of the same order of magnitude the second integral term multiplied by R/ρ_s is negligible so that (22) finally takes the form

$$I^A_{\Gamma(ij)} = R^{\alpha_i-\alpha_j}\int_\theta \Upsilon^{(u)}_i(\theta) f_j(\theta)\mathrm{d}\theta \equiv I_{\Gamma(ij)}, \quad R/\rho_s \to 0. \tag{23}$$

Therefore, the orthogonality property of the eigenfunctions with respect to the contour integral presented in (19) still holds. For detailed explanation of the significance of the orthogonality property for the computation of the GSIFs, the reader is referred to [9, Ch. 12].

3. Numerical examples

The CIM can be implemented in any finite element computer program. However, the error in the computed GSIF is closely related to the error in energy norm, and therefore the choice of the finite element space. The numerical problems discussed in the following were solved by means of a new p-version finite element computer code, called PEGASYS. [1] The analysis presented in Section 2 is verified by the computation of the stress intensity factors for two crack configurations in a cylindrical bar, for which analytical solutions are available, and one inclined crack configuration, for which numerical results from a previous work are reported. The trial space used in the finite element analysis was the trunk space. By definition, the trunk space of degree p spans the set of monomials $\xi^i\eta^j$, $i+j \leqslant p$ augmented by

[1] PEGASYS is a trademark of Engineering Software Research and Development, Inc. 7750 Clayton Road, Suite 204, St. Louis, MO 63117.

the monomial $\xi\eta$ for $p = 1$ and by the monomials $\xi^p\eta$, $\xi\eta^p$ for $p \geqslant 2$ on the standard quadrilateral element defined by $\Omega_{st}^{(q)} = \{\xi, \eta \mid |\xi| \leqslant 1, |\eta| \leqslant 1\}$. In the CIM, the integration was performed along a circle of a radius greater than the radius of the elements at the crack tip. This is because the finite element solution in the first group of elements at the crack tip is not of high accuracy [11].

3.1. Penny-shaped crack imbedded in a cylinder

Consider the domain illustrated in Fig. 2 loaded by traction of magnitude 1.0 in z direction. The solution for this geometry, for $h/b \to \infty$, which is claimed to be accurate to within one percent relative error, is given in [12].

The axisymmetric 2-D solution domain was defined in a parametric form, as illustrated in Fig. 3, such that the values for a, b and h may be easily changed. The finite element mesh surrounding the crack tip contains radial layers graded in a geometric progression in the vicinity of the singular point with the grading factor 0.15. The mesh presented in Fig. 3, for example, has three radial layers. Isotropic material with Young's modulus of 1.0 and Poisson's ratio of 0.3 was used. It is demonstrated in [8] that the stress intensity factors computed by the CIM converge strongly and obviously, and the relative error has the same order of magnitude as the error in the energy norm.

We considered the case $a/b = 1/2$, and computed the normalized stress intensity factor $(K_I/(\sigma\sqrt{\pi a}))$ for several h/b ratios. For $h/b \geqslant 3$ the normalized stress intensity factors remain almost unchanged, so that the values obtained could be correlated with the analytical value available for $h/b = \infty$, which is 0.6881. As the p-level is increased over the elements, the stress intensity factor converges quickly. As an example we show in Fig. 4 the convergence of the stress intensity factor for the three-radial layer

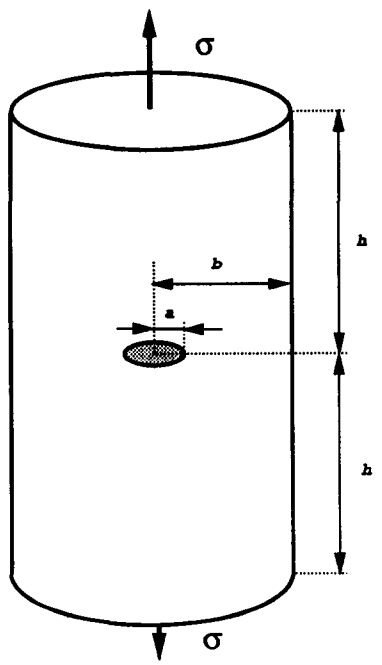

Fig. 2. Penny shaped crack of radius a in a cylinder.

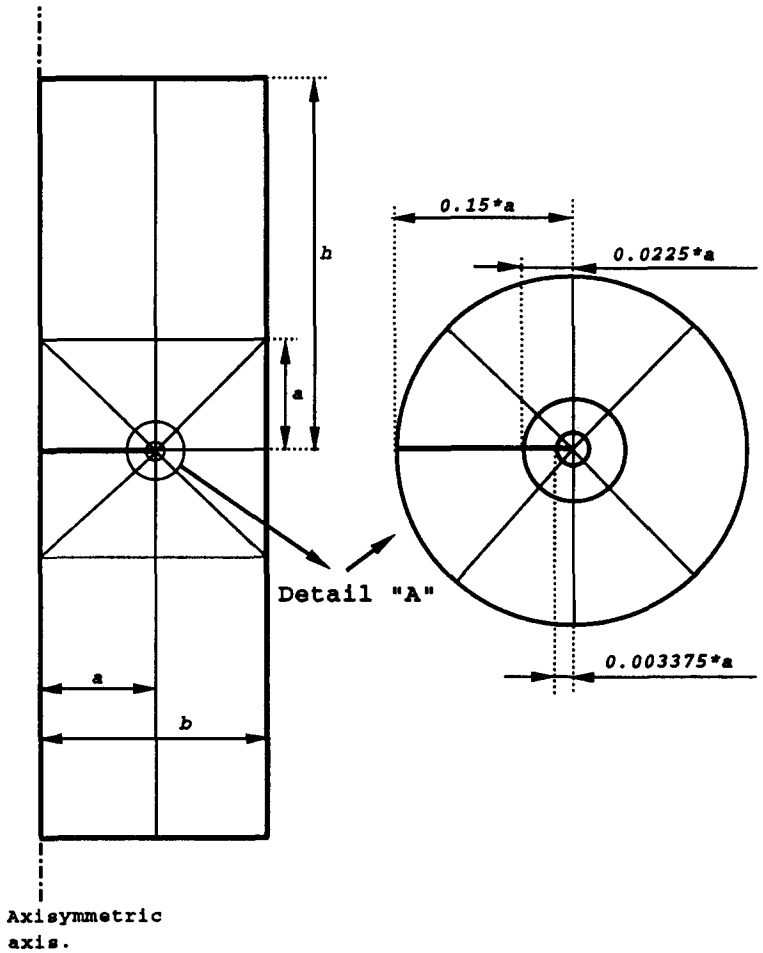

Fig. 3. The 2-D mesh design for the penny shaped crack of radius a.

Table 1
Normalized stress intensity factors computed by the CIM at p-level 8 for various values R/a in a cylinder with $a/b = 1/2$ and $h/b = 3$

R/a	Four-radial layers $\|e\|_E = 0.1\%$ $N = 2849$	Three-radial layers $\|e\|_E = 0.13\%$ $N = 2353$	Two-radial layers $\|e\|_E = 0.28\%$ $N = 1857$
0.0006	0.6857(−0.35%)		
0.001	0.6852(−0.42%)		
0.005	0.6854(−0.39%)	0.6854(−0.39%)	
0.01	0.6851(−0.44%)	0.6850(−0.45%)	
0.05	0.6825(−0.81%)	0.6825(−0.81%)	0.6825(−0.81%)
0.1	0.6801(−1.16%)	0.6801(−1.16%)	0.6801(−1.16%)

Note: The numbers in parentheses represent the relative error from the analytical solution which is 0.6881.

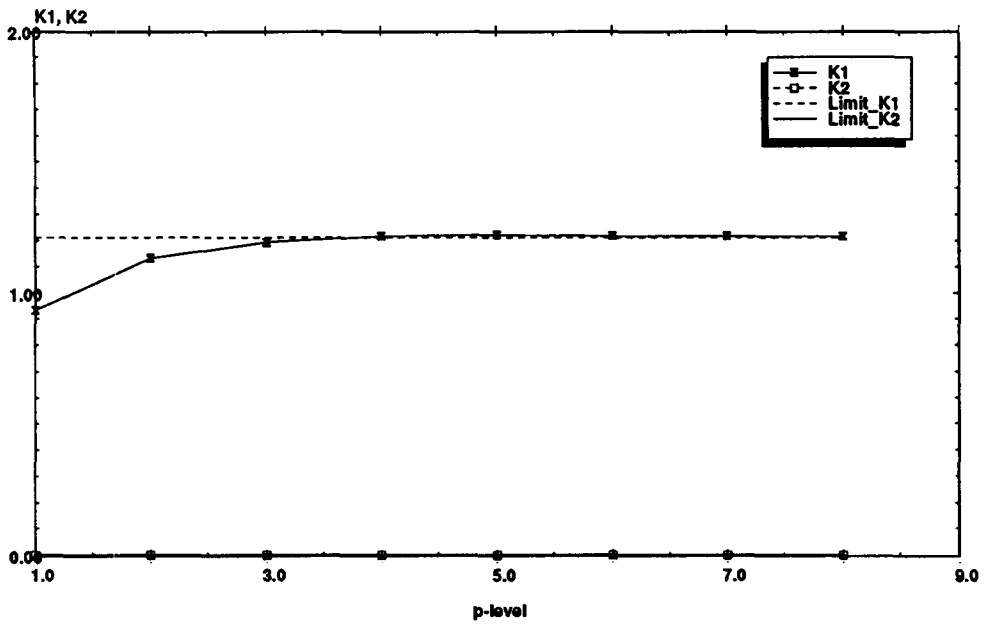

Fig. 4. Stress Intensity Factors for: $R/a = 0.005, a/b = 0.5, h/b = 3$.

mesh model for $R/a = 0.005$. The computed values of the normalized stress intensity factor at $p = 8$ for different values of R/a are listed in Table 1. The number of degrees of freedom is denoted by N. For all cases the mode two stress intensity factor, which is the coefficient corresponding to the first asymptotic term of u_z in (1), was zero as expected.

We see from Table 1 that the stress intensity factors converge to the analytical value for $R/a \to 0$, as predicted by the analysis. Note that even the analytical value may have 1% error.

To improve the quality of the results one may use an extrapolation procedure based on several R/a values, to calculate the stress intensity factor as $R/a \to 0$.

3.2. *Outer crack in a cylinder*

As a second example we consider a cylinder which contains an outer crack propagating toward the axisymmetric axis. The cylinder is loaded by traction of magnitude 1.0 in the z direction, see Fig. 5. The solution for this domain, for $h/b \to \infty$, which is more accurate than 1% (for $a/b < 0.2$ or $a/b > 0.8$), is given in [12]. The axisymmetric finite element mesh is similar to the one shown in Fig. 3, except that the aspect ratio of the elements away from the crack tip is greater because the value $a/b = 0.15$ was chosen. However the elements surrounding the crack tip remain exactly as shown in *Detail A* in Fig. 3. The stress intensity factor for $h/b \geqslant 5$ remains almost unchanged, so that the values obtained could be correlated to the analytical value available for $h/b \to \infty$ which is 21.5325. We demonstrate that even though the error in energy norm is approximately 10% (because of the large aspect ratio of elements away from the crack tip), the values of the stress intensity factor are highly accurate. The computed

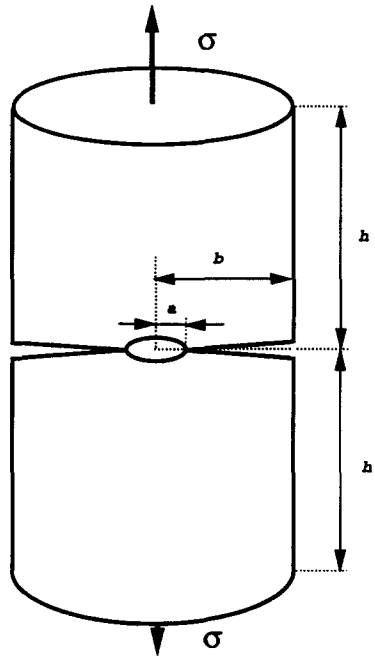

Fig. 5. Outer crack in a cylinder.

Table 2
Stress intensity factors computed by the CIM at p-level = 8 for various values R/a in a cylinder with $a/b = 0.15$ and $h/b = 5$

R/a	Four-radial layers $\|e\|_E = 16.85\%$ $N = 2849$	Three-radial layers $\|e\|_E = 16.86\%$ $N = 2353$	Two-radial layers $\|e\|_E = 16.89\%$ $N = 1857$
0.002	21.5504(0.07%)		
0.0033	21.5553(0.09%)		
0.0166	21.5963(0.28%)	21.5960(0.29%)	
0.033	21.6428(0.5%)	21.6425(0.5%)	21.6402(0.5%)
0.1333	21.9060(1.7%)	21.9056(1.7%)	21.9031(1.7%)

Note: The numbers in parentheses represent the relative error from the analytical solution which is 21.5325.

values for the stress intensity factor at $p = 8$ for the different values of R/a are listed in Table 2. For all cases $K_{II} = 0$ as expected.

3.3. *Inclined crack in a cylinder*

The two example problems just discussed were constructed so that only the first symmetric term in the asymptotic expansion was nonzero. This permitted us to examine the performance of the contour integral method in comparison with known exact solutions. In practical problems no such restrictions

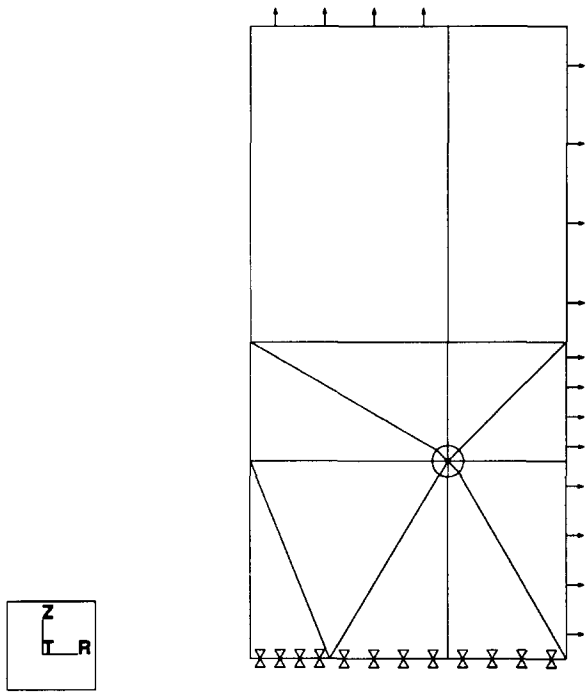

Fig. 6. Inclined crack in a cylinder: finite element mesh.

apply and the exact solution is not known. The following test problem is more nearly representative of practical problems, and was discussed in [13].

In this problem the cylinder has a radius of 2 units and a length of 4 units. The crack mouth is located at the $z = 0$ axis at a radius of 0.5 units from the z-axis. The crack tip has the coordinates of $r = 1.25$ units, and $z = 1.25$ units (such that the crack inclination angle is 59.036°). The applied stress of unit magnitude is acting on the cylinder's entire outer radius and is also applied to the portion of the end of the cylinder which is defined by $0 < r < 1.25$ units. Note that a singular point also exists where the load at the end of the cylinder is interrupted. The Young modulus was taken to be 1 and Poisson's ratio 0.3.

The finite element mesh used in our computations, having three refined radial layers around the crack tip, is shown in Fig. 6. The computed values for the stress intensity factors for different values of R are listed in Table 3.

The results reported in [13] for the stress intensity factors are $K_{\mathrm{I}} = 1.024597$ and $K_{\mathrm{II}} = -0.11470$. The J-integral value computed by these stress intensity factors is 0.9673. The average value for the J-integral computed independently of the stress intensity factors in [13] is 1.0277. To verify the results, we have computed the J-integral based on the stress intensity factors reported in Table 3, and independently, we computed the J-integral based on the energy release rate. All four values for the J-integral are summarised in Table 4.

As noticed, our results are very close for both independent methods used to compute the J-integral, and correspond closely with the J-integral computed directly in [13].

Table 3
Stress intensity factors for the inclined crack problem, computed by the CIM for various values R

R	$\|e\|_E = 1.61\%$ $N = 2264$ K_I	K_{II}
0.0035	1.053707	−0.151491
0.0050	1.060002	−0.152609
0.0100	1.064110	−0.155383
0.0400	1.077022	−0.166896
0.0900	1.089741	−0.184680

Table 4
J-integral values for the inclined crack problem

Based on SIFs for $R = 0.0035$	Based on ERR estimated at $p = \infty$	Based on SIFs [13]	Direct [13]
1.031	1.022	0.967	1.028

Note: SIF = Stress intensity factor; ERR = Energy release rate.

4. Summary and conclusions

The understanding of the behaviour of the solution for a 2-D axisymmetric domain in the neighborhood of a singular point is an important requirement in the failure analysis of many important practical problems arising in connection with the analysis of pressure vessels and piping systems in nuclear and mechanical engineering. We have shown in this paper that the eigenpairs in the vicinity of *any* singular point of a 2-D axisymmetric body are identical to their plane strain counterparts in the framework and under the assumptions of linear elastic fracture mechanics theory.

The Steklov weak formulation was used for finding the eigenpairs which characterize the solution in the vicinity of the singular boundary points, and an auxiliary function was developed for the extraction of the stress intensity factors for crack configurations. The CIM was then applied to extract these stress intensity factors, providing both K_I and K_{II}. The rate of convergence of K_I and K_{II} is comparable to the rate of convergence of the strain energy. Therefore the method of extraction is superconvergent.

The results of the numerical experiments were presented to support our analysis. The method of extraction for the computation of GSIFs in 2-D domains, presented in [8], has been extended for application to the axisymmetric case.

Acknowledgements

This research work has been supported by the Air Force Office of Scientific Research under Grant F49620-93-1-0173. This support is gratefully acknowledged.

Special thanks are given to Dr. R.L. Actis for his assistance with implementation of the algorithm described herein into PEGASYS.

References

[1] P. Grisvard, *Elliptic Problems in Nonsmooth Domain*, Pitman, London, UK, 1985.
[2] D. Leguillon and E. Sanchez-Palencia, *Computation of Singular Solutions in Elliptic Problems and Elasticity*, Wiley, New York, 1987.
[3] Z. Yosibash and B.A. Szabo, "Numerical analysis of singular points", in: P.K. Basu and A. Nagar (eds.), *Recent Developments in Computational Mechanics*, AD-Vol. 39, ASME press, New York, pp. 29–44, 1993.
[4] Z. Yosibash, Numerical analysis of singularities and first derivatives for elliptic boundary value problems in two dimensions, Doctoral Dissertation, Sever Institute of Technology, Washington University, Missouri, August 1994.
[5] P. Papadakis, Computational aspects of the determination of the stress intensity factors for two-dimensional elasticity, Ph.D. Dissertation, University of Maryland, 1988.
[6] A.R. Zak, "Stresses in the vicinity of boundary discontinuities in bodies of revolution", *J. Appl. Mech.* **31**, pp. 150–152, 1964.
[7] I. Babuska and A. Miller, "The post processing approach in the finite element method-part 2: The calculation of stress intensity factors", *Int. J. Numer. Methods Eng.* **20**, pp. 1111–1129, 1984.
[8] B.A. Szabo and I. Babuska, "Computation of the amplitude of stress singular terms for cracks and reentrant corners", in: T.A. Cruse (ed.), *Proc. 19th Symp. on Fracture Mechanics*, ASTM STP 969, ASTM, Philadelphia, pp. 101–124, 1988.
[9] B.A. Szabo and I. Babuska, *Finite Element Analysis*, Wiley, New York, 1991.
[10] I.N. Sneddon, "The distribution of stress in the neighborhood of a crack in an elastic solid", *Proc. R. Soc. London Ser. A* **187**, pp. 229–260, 1946.
[11] K. Izadpanah, Computation of stress components in the P-version of the finite element method, D.Sc. dissertation, Washington University, 1984.
[12] H. Tada, P. Paris and G. Irwin, The Stress Analysis of Cracks Handbook, Paris Productions Inc. and Del Research Corporation, 1985.
[13] H.F. Nied, "A note on axisymmetric J-integrals", *J. Appl. Mech.* **61**, pp. 214–217, 1994.